

PACS numbers: 42.55.Ks; 42.60.By
DOI: 10.1070/QE2009v039n11ABEH014085

Development of a chemical oxygen – iodine laser with production of atomic iodine in a chemical reaction

M. Čenský, O. Špalek, V. Jirásek, J. Kodymová, I. Jakubec

***Abstract*. The alternative method of atomic iodine generation for a chemical oxygen – iodine laser (COIL) in chemical reactions with gaseous reactants is investigated experimentally. The influence of the configuration of iodine atom injection into the laser cavity on the efficiency of the atomic iodine generation and small-signal gain is studied.**

Keywords: *chemical oxygen – iodine laser, generation of atomic iodine.*

1. Introduction

A chemical oxygen – iodine laser (COIL) emits in the near-IR region at the 1.315-μm electronic transition in the iodine atom

$$\mathrm{I}(^2\mathrm{P}_{1/2}) \rightarrow \mathrm{I}(^2\mathrm{P}_{3/2}) + h\nu. \quad (1)$$

Due to the energy transfer from the $\mathrm{O}_2(^1\Delta_g)$ state of singlet oxygen molecules to iodine atoms, iodine atoms in the excited electronic state are produced:

$$\mathrm{O}_2(^1\Delta_g) + \mathrm{I}(^2\mathrm{P}_{3/2}) \rightarrow \mathrm{O}_2(^3\Sigma_g) + \mathrm{I}(^2\mathrm{P}_{1/2}). \quad (2)$$

In a conventional COIL, atomic iodine used for lasing is produced during the dissociation of molecular iodine interacting with singlet oxygen. In this process, the energy of several $\mathrm{O}_2(^1\Delta_g)$ molecules is spent on dissociation of one I_2 molecule. Thus, these $\mathrm{O}_2(^1\Delta_g)$ molecules are lost for pump reaction (2)

$$\mathrm{I}_2 + n\,\mathrm{O}_2(^1\Delta_g) \rightarrow 2\,\mathrm{I} + n\,\mathrm{O}_2(^3\Sigma_g)\ (n = 4-6). \quad (3)$$

It is obvious that employing another method of atomic iodine production without the consumption of the $\mathrm{O}_2(^1\Delta_g)$ energy will make it possible not only to save this energy, but also will provide other advantages, for example, suppression of the fast quenching of exited iodine atoms I* by I_2 molecules

$$\mathrm{I}^* + \mathrm{I}_2 \rightarrow \mathrm{I} + \mathrm{I}_2,\ \ k_4 = 3.1\times10^{-11}\ \mathrm{cm}^3\ \mathrm{s}^{-1}. \quad (4)$$

We assume that direct generation of atomic iodine in the laser medium will eliminate the above disadvantages in the usage of I_2, and probably, will increase the laser efficiency. Several laboratories published their results on the use of different configurations and technologies of discharge dissociation of iodine atom donors. The review of these publications was presented by Schmiedberger et al. in [1]. The idea of our paper is based on the chemical generation of atomic iodine from suitable gaseous reactants injected into the singlet oxygen flow. Two chemical processes were suggested involving the fast reaction of hydrogen iodide with either chlorine or fluorine atoms produced in preliminary chemical reactions [2 – 9].

First, we studied the system with chlorine atoms, which provided the atomic iodine yield up to ~ 80 % and was tested in a supersonic COIL. The small-signal gain of 0.4 % cm^{-1} and the laser output power up to 450 W were obtained. In these experiments, all reacting gases were admixed into the subsonic $\mathrm{O}_2(^1\Delta_g)$ flow (upstream the nozzle throat). The chemical efficiency of this COIL configuration did not exceed that of a conventional COIL, which was, probably, caused by some undesirable reactions between some reaction components and $\mathrm{O}_2(^1\Delta_g)$. To avoid these reactions, we suggested generating atomic iodine in two separate (side) reactors, and then injecting it into the primary flow with $\mathrm{O}_2(^1\Delta_g)$. In this paper, we measured the atomic iodine yield in reactions with Cl atoms and the gain for different configurations of reactant injectors.

2. System of reactions

The production of iodine atoms proceeds in two successive stages. First, atomic chlorine is formed in the fast reaction of gaseous chlorine dioxide with nitrogen oxide

$$\mathrm{ClO}_2 + 2\,\mathrm{NO} \rightarrow \mathrm{Cl} + 2\,\mathrm{NO}_2, \quad (5)$$

and then the Cl atoms react with gaseous hydrogen iodide generating iodine atoms in the reaction

$$\mathrm{Cl} + \mathrm{HI} \rightarrow \mathrm{HCl}\,(\mathrm{HCl}^*) + \mathrm{I}, \quad (6)$$
$$k_6 = 1.64\times10^{-10}\ \mathrm{cm}^3\ \mathrm{s}^{-1}.$$

Besides these two principal reactions, the recombination reactions of chlorine and iodine atoms are responsible for the loss of these atoms:

M.Čenský, O.Špalek, V.Jirásek, J.Kodymová Institute of Physics, Academy of Sciences CR, Na Slovance 2, 182 21 Prague, Czech Republic; e-mail: kodym@fzu.cz;
I.Jakubec Institute of Inorganic Chemistry, Academy of Sciences CR, 250 68 Řež, Czech Republic

Received 5 February 2009; revision received 24 April 2009
Kvantovaya Elektronika **39** (11) 1023 – 1027 (2009)
Submitted in English

$$Cl + NO_2 + N_2 \rightarrow ClNO_2 + N_2, \quad (7)$$
$$k_7 = 7.2\times10^{-31}\ cm^6\ s^{-1},$$

$$ClNO_2 + Cl \rightarrow Cl_2 + NO_2, \quad (8)$$
$$k_8 = 3.0\times10^{-11}\ cm^3\ s^{-1},$$

$$I + NO_2 + N_2 \rightarrow INO_2 + N_2, \quad (9)$$
$$k_9 = 1.4\times10^{-31}\ cm^6\ s^{-1},$$

$$I + INO_2 \rightarrow I_2 + NO_2, \quad (10)$$
$$k_{10} = 8.3\times10^{-11}\ cm^3\ s^{-1},$$

$$I + NO + N_2 \rightarrow INO + N_2, \quad (11)$$
$$k_{11} = 1.8\times10^{-32}(T/298)^{-1}\ cm^6\ s^{-1},$$

$$I + INO \rightarrow I_2 + N_2, \quad (12)$$
$$k_{12} = 2.6\times10^{-10}\ cm^3\ s^{-1},$$

$$I + I + N_2 \rightarrow I_2 + N_2, \quad (13)$$
$$k_{13} = 6.15\times10^{-34}(T/298)^{0.07}e^{(7433/RT)}\ cm^6\ s^{-1},$$

$$I + I + HI \rightarrow I_2 + HI, \quad (14)$$
$$k_{14} = 8.13\times10^{-32}(T/298)^{-3.5}\ cm^6\ s^{-1}.$$

Iodine atoms can also recombine on the walls

$$I + I + wall \rightarrow I_2 + wall, \quad (15)$$
probability $\gamma_{15} = 1.0$.

The system of reactions is described in detail in papers [2, 3, 8, 9], which present references on the rate constants. A computational modeling of the whole system of reactions assisted at designing the experimental configuration for injection of individual reactants in the iodine reactors, and helped to interpret the experimental results.

3. Experimental setup

Figure 1 shows the scheme of the experimental setup employed to study a system with two side reactors for the atomic iodine generation and its injection into the supersonic nozzle region. Each reactor (*1*) consists of a rectangular housing with the ClO_2 inlet (*3*), the NO injector (*4*), and the HI injector (*5*). In this case, the injection of NO and HI is termed the NO – HI order. In some experiments, we also used the reverse injection of these gases and termed it the HI – NO order (see Fig. 2a). Each NO injector consisted of 16 holes with a diameter 0.4 mm arranged in two rows, and the HI injector consisted of 16 holes with a diameter 0.3 mm arranged in two rows. Both rows in each injector formed the 60° angle to the primary flow direction (*2*). Injectors (*4*) and (*5*) were tested also in three mutual positions (Fig. 2b) to determine the optimal mixing of both reactants. Generated atomic iodine was injected from the reactors into the laser nozzle (sonic injection) through 16 openings with a diameter 2.3 mm arranged in one row and 15 openings with a diameter 0.8 mm arranged in one row. All the holes were directed at the angle of 60° to the nozzle wall. The rows of larger openings and smaller openings were located 2 mm and 3.2 mm, respectively, from the nozzle throat. To increase the penetration of the secondary gas with iodine atoms into the primary flow, in later experiments every other larger opening 0.8 mm in diamter was plugged. In addition, all the remaining openings had a conical shape to attain a supersonic injection of the secondary gas. The diameters of the larger openings were

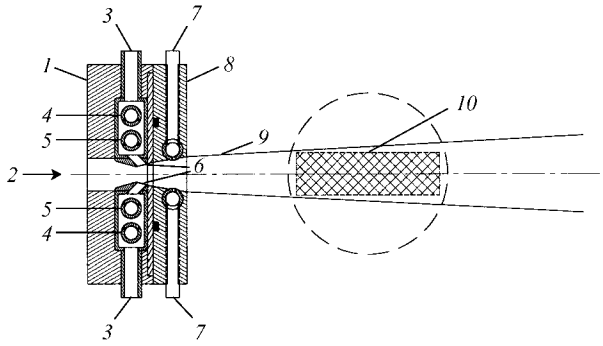

Figure 1. Cross section of the COIL cavity with a supersonic nozzle and two side reactors for chemical generation of atomic iodine in reactions with Cl atoms:
(*1*) reactor body; (*2*) primary flow with $O_2(^1\Delta_g)$; (*3*) inlet of the (ClO_2 – N_2) mixture; (*4*) NO injectors; (*5*) HI injectors; (*6*) injection of I atoms; (*7*) inlet of tertiary N_2; (*8*) housing of the 'tertiary' N_2 injector; (*9*) supersonic cavity region, (*10*) gain diagnostic region.

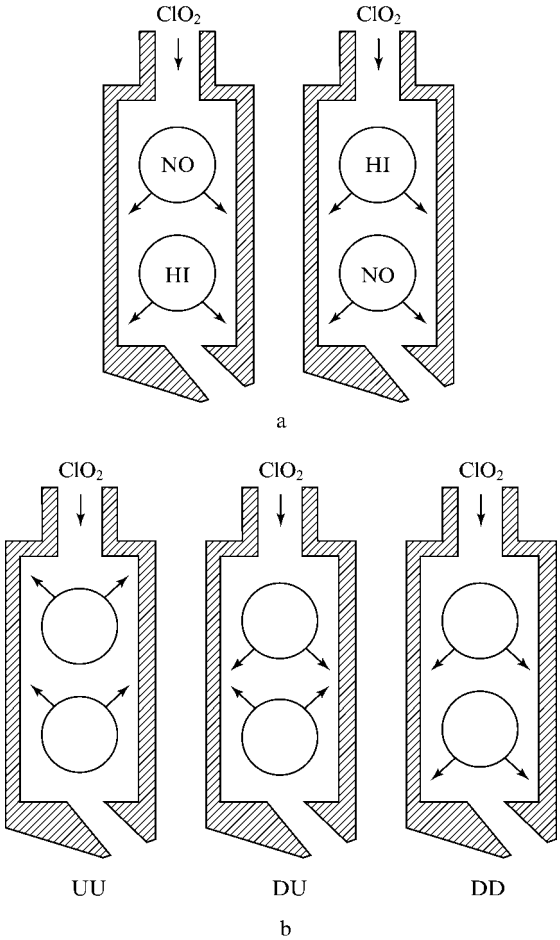

Figure 2. Injection order of NO and HI reactants into ClO_2 flow (a) and three different positions of NO and HI injectors (UU – injection directed up-up, DU – down-up, DD – down-down) (b).

from 2.5 mm to 3.1 mm and the diameters of the smaller openings were from 0.8 mm to 0.9 mm. Injector (*8*) in Fig. 1 served for introducing additional 'tertiary' nitrogen. A critical cross section of the nozzle throat was 50 mm × 5 mm.

Undiluted nitrogen oxide and HI were used because the diluting gas significantly accelerates the ternary loss reactions (7), (9), (11)–(13), (14). Chlorine dioxide was diluted with nitrogen in the ratio 1:10 for the safety reasons. The concentration of atomic iodine and the gas temperature were measured by means of the Iodine Scan Diagnostics (ISD) method [10] based on the near-IR spectroscopy. This method employed a narrowband tunable probe diode laser to monitor the radiation absorption or gain on transition (1) at 1.315 μm. The ISD probe beam was directed perpendicularly to the cross-section plane in Fig. 1 and was moved either along the gas flow or perpendicularly to the flow to measure the profile of the atomic iodine concentration or gain. These profiles in the horizontal direction were recorded at distances of 52–86 mm from the throat, and in the vertical direction – in the interval of 8 mm below and above the nozzle axis.

4. Results and discussion

4.1 Generation of atomic iodine in side reactors and its injection into a supersonic flow of the N_2–He mixture

NO–HI injection order. In this configuration, the density of atomic iodine across the laser cavity (perpendicularly to the gas flow direction) was initially very inhomogeneous due to insufficient mixing of injected iodine with the primary gas flow. This situation was improved by introducing the 'tertiary' nitrogen (N_2^{tert}) into the supersonic region downstream the reactor. The influence of N_2^{tert} on the iodine concentration profiles is shown in Fig. 3. One can see that N_2^{tert} favours the homogenization of the iodine concentration in the cavity, and also influences the production rate of iodine atoms, which slightly increases with increasing the N_2^{tert} flow rate. However, the addition of N_2^{tert} reduces the Mach number of the gas stream in the cavity, which results in some increase in the gas temperature. In this experimental setup, the maximum atomic iodine yield related to the initial ClO_2 flow rate was 40 %.

The effect of NO flow rate on the atomic iodine yield at different HI flow rates was measured in the 'DD' injector position (see Fig. 2b). It was found that when the NO flow rate was increased, the concentration of atomic iodine increased almost linearly and reached a maximum at the ratio $[NO]/[ClO_2] = 3.3$. This value is higher than the ratio of 2 corresponding to stoichiometry of reaction (5). The HI flow rate did not affects the change in the atomic iodine concentration, which indicates that it is the production of Cl atoms that was the main factor controlling the rate of reactions under these experimental conditions [1.5 mmol s^{-1} (ClO_2), 1.5–6.5 mmol s^{-1} (NO), 0.9–1.9 mmol s^{-1} (HI), 'DD' position of injectors]. The maximum iodine concentration of 5×10^{14} cm^{-1} and the atomic iodine yield up to 55 % with respect to the ClO_2 concentration were attained. According to the results of simplified 2D modeling, the dimensions of some regions with a high local concentration of Cl and a low concentration of HI can increase in the case of the NO–HI injection order (near the NO jet), resulting in acceleration of the ternary loss-reactions of Cl atoms.

An increase in the ClO_2 flow rate from 1.5 to 2.3 mmol s^{-1} at the constant ratio $[NO]/[ClO_2] = 2$ leads to a decrease in the yield of iodine atoms from 40 % to 26 %. This can be explained by an increase in the recombination rate of Cl and I atoms due to the pressure growth in the reactor, caused by an increase in the 'secondary' nitrogen in the ClO_2/N_2 mixture.

HI–NO injection order. Figure 4 presents an example of the concentration profiles of atomic iodine across the cavity, measured in the case of the HI–NO injection order in the 'UU' position of injectors for the 2.3-mmol s^{-1} ClO_2 flow rate at different flow rates of HI. The comparison of Figs 3 and 4 shows that the yield of atomic iodine was substantially higher in this experimental configuration than in the case of the NO–HI injection order, approaching virtually 100 % under optimal conditions. A very high density of iodine atoms [$(1.35–1.85)\times10^{15}$ cm^{-3}] was measured at the following flow rates: 2.3 mmol s^{-1} (ClO_2), 7.5 mmol s^{-1} (NO), 3 mmol s^{-1} (HI), 37 mmol s^{-1} (N_2^{tert}), and ~ 80 mmol s^{-1} (He) and

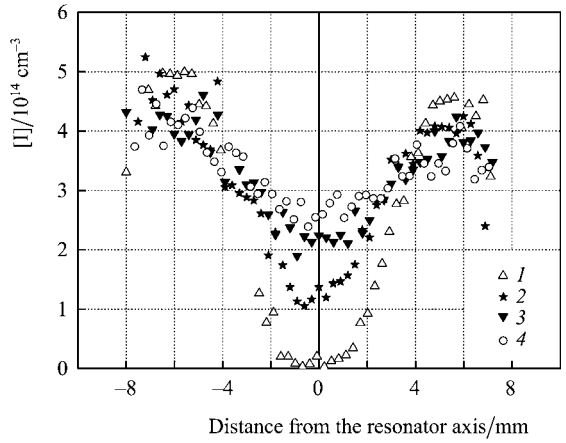

Figure 3. Concentration profiles of atomic iodine across the laser cavity (position 0 is the cavity center) at N_2^{tert} flow rates: 0 (*1*); 12 (*2*); 20 (*3*); 27 (*4*); at primary gas flow rates: 79 (He) + 22 (N_2); at flow rates in the side reactors: 1.5 (ClO_2) + 13 (N_2), 3 (NO), and 1.85 (HI) (in mmol s^{-1}); NO–HI injection order, UU position of injectors.

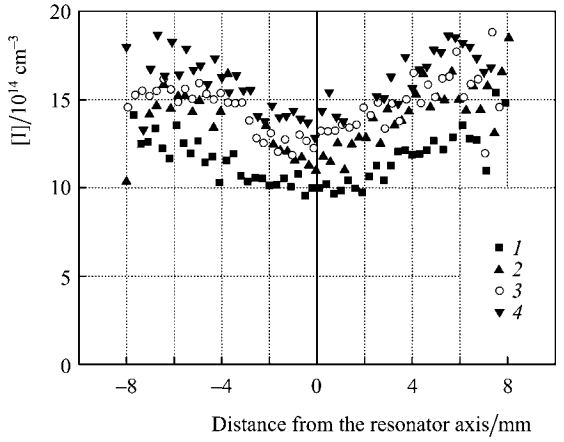

Figure 4. Concentration profile of atomic iodine across the laser cavity at different flow rates of HI and NO in the side reactors (in mmol s^{-1}): 1.34 (HI) + 6.6 (NO) (*1*); 2.3 (HI) + 6.6 (NO) (*2*); 2.95 (HI) + 6.6 (NO) (*3*); 3.0 (HI) + 7.55 (NO) (*4*), and 2.3 (ClO_2 + 33 (N_2^{tert}); primary gas flow rate: 22 (N_2) + 80 (He); HI–NO injection order, UU position of injectors.

~ 22 mmol s^{-1} (N_2) in the primary flow. The production rate of iodine atoms increased linearly with increasing both NO and HI flow rates in the given flow rate range.

The higher yield of atomic iodine in the case of the HI – NO order can be explained by a higher fraction of Cl atoms produced at a low pressure in the supersonic nozzle region, where the ternary loss-reactions are suppressed. The modeling of reaction kinetics showed that the Cl atoms are formed in a shorter time in this injection order compared to the NO – HI order and, hence, the ClO production is slower due to an instantaneous consumption of Cl atoms by reaction with HI molecules [reaction (6)]. Therefore, the ClO concentration produced during the reaction

$$ClO_2 + Cl \rightarrow 2ClO,\ k_{16} = 5.8\times10^{-11}\ cm^3\ s^{-1}, \qquad (16)$$

decreases as does the overall rate of Cl atoms production in reaction (5) (see details in paper [1]). This results in generation of larger fractions of Cl and I atoms outside the reactor (only in the supersonic region), where the pressure and the loss of both Cl and I atoms are lower.

Most experiments with the supersonic injection of atomic iodine were performed using the HI – NO injection order. It was found that the penetration of the supersonically injected secondary gas with atomic iodine into the primary flow was much more efficient than in the case of sonic injection. The concentration of I atoms across the cavity was rather homogeneous (except for boundary layers) and attained up to 14×10^{14} cm^{-3}. 'Tertiary' nitrogen N_2^{tert} enhanced the iodine production and more homogeneous atomic iodine concentration profile was achieved. However, N_2^{tert} reduced the Mach number from 2.3 to 1.8 in the cavity center, which caused an increase in the gas temperature by ~ 100 K. The yield of atomic iodine was above 60 % and reached even 100 % in some cases.

4.2 Small signal gain measurements

The small signal gain was measured in the configuration with supersonic injection of atomic iodine at both NO – HI and HI – NO injection orders and with all three positions of NO and HI injectors (Fig. 2b). In measuring the gain, nitrogen in the primary flow was replaced by a gas containing singlet oxygen $O_2(^1\Delta_g)$ obtained in a chemical jet generator by means of a well-known reaction of chlorine with hydrogen peroxide in an alkaline solution. The design of this generator is described in detail in paper [11]. The efficiency of the $O_2(^1\Delta_g)$ generator determined by $Y_\Delta U_{Cl}$ – the product of the $O_2(^1\Delta_g)$ yield and the Cl_2 utilisation coefficient, was equal to 0.62.

HI – NO injection order. First, the measurements for the HI – NO order were performed. An example of the gain dependence on the HI flow rate is shown in Fig. 5. It was found that the orientation of the injectors (DD or UU) had no significant effect on the gain. The maximum gain was achieved at the ratio $[HI]/[ClO_2] \sim 0.6$, and then the gain fell down to zero with increasing this ratio. We observed the light absorption on transition (1) accompanied by a sudden temperature rise. This effect was explained by a low fraction of HI molecules consumed in reaction (6) in the side reactors. The unreacted HI then flowed into the cavity where it reacted with $O_2(^1\Delta_g)$ according to (17), thereby probably producing the radical $HO_2^\bullet$:

$$HI + O_2(^1\Delta_g) \rightarrow HO_2^\bullet + I\,. \qquad (17)$$

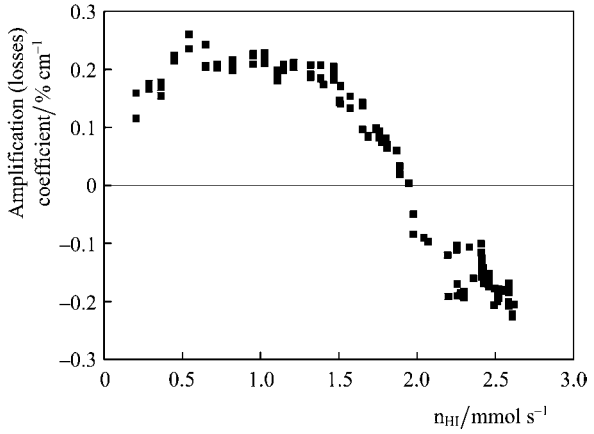

Figure 5. Dependence of the gain (loss) on the HI flow rate (measured in the region located in the resonator cross section 4 mm below its axis). Gas flow rates into the $O_2(^1\Delta_g)$ generator (in mmol s^{-1}): 100 (He) + 22 (Cl_2); flow rates in the side reactors (in mmol s^{-1}): 1.5 (ClO_2) + 13 (N_2), 3.5 (NO); HI – NO injection order, UU position of injectors.

The $O_2(^1\Delta_g)$ quenching rate by the $HO_2^\bullet$ radical is very high [12] ($k_{HO_2} = 3.3\times10^{-11}$ cm^3 s^{-1}), which confirms our hypothesis about the negative role of $HO_2^\bullet$ radicals. A significant heat release accompanying the formation of atomic iodine in the $HI/O_2(^1\Delta_g)$ mixture was observed in our earlier experiments in the absence of ClO_2 and NO, i.e. without Cl atoms in the reaction system [4]. This confirms our hypothesis about the presence of $HO_2^\bullet$ radicals in the gas flow and their negative effect on the process under study.

NO – HI injection order. The small-signal gain with a peak value of 0.38 % cm^{-1} in the cavity center was achieved in this experimental configuration. As follows from Fig. 6, due to the penetration of injected iodine into the primary flow, the small-signal gain profile was rather homogeneous (except for the boundary layers). The profile became inhomogeneous at higher He flow rates in the primary stream (100 mmol s^{-1}) and lower HI flow rates (1 – 1.5 mmol s^{-1}) due to a weaker penetration of the secondary flow into the cavity. In this case, the measured gain was minimal in the cavity centre.

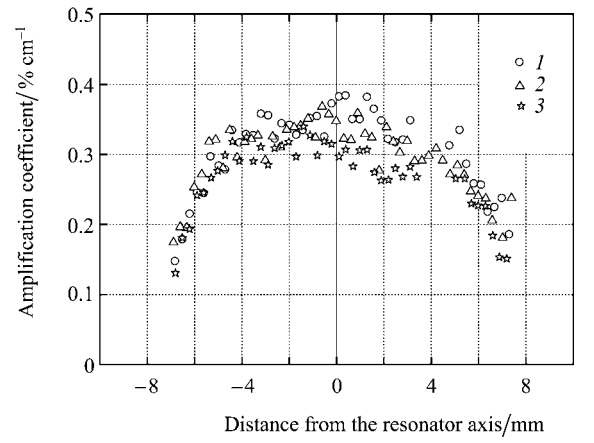

Figure 6. Small-signal gain profile across the laser cavity at different HI and Cl_2 flow rates: 2.2 (HI) + 29.5 (Cl_2) (*1*), 3.05 (HI) + 29 (Cl_2) (*2*), 3.0 (HI) + 24.5 (Cl_2); other flow rates: 60 (He), 1.5 (ClO_2), 6 (NO) (in mmol s^{-1}); NO – HI injection order, DD position of injectors.

Assuming that $O_2(^1\Delta_g)$ is quenched by the $HO_2^{\bullet}$ radicals, we used DI instead of HI to measure the gain in some experiments. We supposed that the $DO_2^{\bullet}$ radical is a weaker quencher of $O_2(^1\Delta_g)$ than $HO_2^{\bullet}$. This assumption was not confirmed because the values of the gains obtained using HI and DI proved close. An example of the gain dependence on the DI flow rate is shown in Fig. 7. The gain initially increased with increasing DI flow rate, reached its maximum, and then decreased, probably due to reaction (17). This indicates that the atomic iodine generation in the setup with two side reactors was inefficient because of insufficient HI (DI) consumption in the reactors and, hence, because of the quenching of $O_2(^1\Delta_g)$ by some reaction products, probably the $HO_2^{\bullet}$ ($DO_2^{\bullet}$) radicals in the primary flow of the COIL. A similar problem was previously observed in a setup with the direct subsonic mixing of reaction gases in the primary flow; however, this problem was not completely solved even when separate reactors were used to generate atomic iodine.

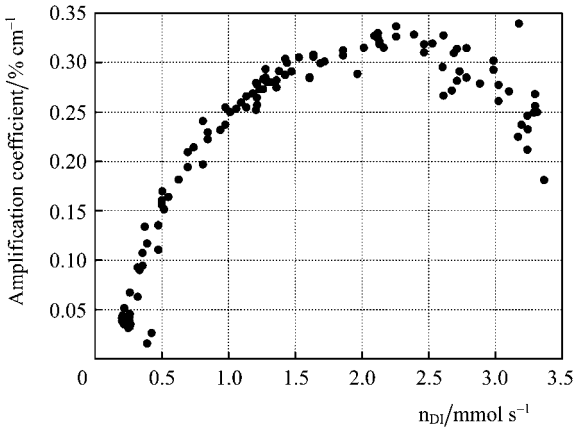

Figure 7. Dependence of the small-signal gain on the DI flow rate (measured in the region located in the resonator cross section 4 mm below its axis). Gas flow rates of the primary gas (in mmol s^{-1}): 87 (He) + 30 (Cl_2); flow rates in the side reactors (in mmol s^{-1}): 1.1 (ClO_2), 3.1 (NO); NO–HI injection order, DD position of injectors.

5. Conclusions

We have studied the chemical generation of atomic iodine in a supersonic COIL. The system consisted of two separate side reactors for atomic iodine production in the reaction of Cl atoms with HI molecules. The reactors were attached to the laser cavity and were employed to inject secondary gas with iodine atoms into the primary flow either in the sonic or supersonic regimes.

The concentration profiles of generated iodine atoms across the cavity and the small-signal gain were substantially affected by the position of HI and NO injectors in the reactors and by the additional supersonic injection of nitrogen downstream the laser nozzle throat. The maximum iodine concentration in the optical resonator was very high, 1.8×10^{15} cm^{-3}, which was almost twice higher than in the previously used subsonic mixing of reactants (ClO_2, HI and NO) upstream the nozzle throat. The maximum yield of iodine atoms (related to ClO_2 flow rate) was virtually 100 % under the optimal conditions.

In the gain measurements performed with $O_2(^1\Delta_g)$ in the primary flow, both HI–NO and NO–HI injection orders and different positions of NO and HI injectors were tested. The maximum gain was 0.38 % cm^{-1}, which is a rather unsatisfactory result. The use of the side reactors for atomic iodine generation with its subsequent injection into the laser cavity had no significant advantages compared to the direct mixing of reaction gases (ClO_2, NO, and HI) in the primary flow with $O_2(^1\Delta_g)$. The reason was obviously an insufficient HI consumption in the side reactors with a partial penetration of HI into the primary flow, and the quenching of $O_2(^1\Delta_g)$ by some reaction product of HI oxidation.

Acknowledgements. This work was supported by the USAF European Office for Research and Development (Grant No. FA8655-05-M4027) and the Grant Agency of the Czech Republic (Grant No. 202/05/0359). This investigation performed within the framework of the Institutional Research Plan AVOZ 10100523 of the Institute of Physics, Academy of Sciences of the Czech Republic.

References

1. Schmiedberger J., Jirásek V., Kodymová J., Rohlena K. *AIAA Paper*, 2007-4239 (2007).
2. Jirásek V., Špalek O., Kodymová J., Čenský M. *Chem. Phys.*, **269**, 167 (2001).
3. Špalek O., Jirásek V., Čenský M., Kodymová J., Jakubec I., Hager G.D. *Chem. Phys.*, **282**, 147 (2002).
4. Špalek O., Čenský M., Jirásek V., Kodymová J., Jakubec I., Hager G.D. *IEEE J. Quantum Electron.*, **40**, 564 (2004).
5. Kodymová J., Špalek O., Jirásek V., Čenský M., Jakubec I., Hager G.D. *Appl. Phys. A*, **77**, 331 (2003).
6. Špalek O., Jirásek V., Čenský M., Kodymová J., Jakubec I., Hager G.D. *Proc. SPIE Int. Soc. Opt. Eng.*, **5777**, 181 (2004).
7. Špalek O., Jirásek V., Čenský M., Kodymová J., Jakubec I. *AIAA Paper*, 2005-5170 (2005).
8. Jirásek V., Špalek O., Čenský M., Picková I., Kodymová J., Jakubec I. *Chem. Phys.*, **334**, 167 (2007).
9. Jirásek V., Čenský M., Špalek O., Kodymová J., Picková I., Jakubec I. *Chem. Phys.*, **345**, 14 (2008).
10. Tate R.F., Hunt B.S., Helms C.A., Truesdell K.A., Hager G.D. *IEEE J. Quantum Electron.*, **31**, 1632 (1995).
11. Kodymová J., Špalek O. *Jpn. J. Appl. Phys.*, **37**, 117 (1998).
12. Podolske J.R., Johnston H.S. *J. Phys. Chem.*, **87**, 628 (1983).